

Pharmaceutical Nanotechnology

Hypericin-loaded nanoparticles for the photodynamic treatment of ovarian cancer

Magali Zeisser-Labou  be, Norbert Lange, Robert Gurny, Florence Delie*

Department of Pharmaceutics and Biopharmaceutics, School of Pharmaceutical Sciences, University of Geneva, University of Lausanne, 30 Quai E. Ansermet, CH-1211 Geneva 4, Switzerland

Received 17 May 2006; received in revised form 6 July 2006; accepted 7 July 2006

Available online 15 July 2006

Abstract

A photodynamic approach has been suggested to improve diagnosis and therapy of ovarian cancer. As Hypericin (Hy), a natural photosensitizer (PS) extracted from *Hypericum perforatum*, has been shown to be efficient *in vitro* and *in vivo* for the detection or treatment of other cancers, Hy could also be a potent tool for the treatment and detection of ovarian cancer. Due to its hydrophobicity, systemic administration of Hy is problematic. Thus, polymeric nanoparticles (NPs) of polylactic acid (PLA) or polylactic-co-glycolic acid (PLGA) were used as a drug delivery system. Hy-loaded NPs were produced with the following characteristics: (i) size in the 200–300 nm range, (ii) negative zeta potential, (iii) low residual PVAL and (iv) drug loading from 0.03 to 0.15% (w/w). Their *in vitro* photoactivity was investigated on the NuTu-19 ovarian cancer cell model derived from Fischer 344 rats and compared to free drug. Hy-loaded PLA NPs exhibited a higher photoactivity than free drug. Increasing light dose or incubation time with cells induced an enhanced activity of Hy-loaded PLA NPs. Increased NP drug loading had a negative effect on their photoactivity on NuTu-19 cells: at the same Hy concentration, the higher was the drug loading, the lower was the phototoxic effect. The influence of NP drug loading on the Hy release from NPs was also investigated.

  2006 Elsevier B.V. All rights reserved.

Keywords: Photodynamic therapy; Biodegradable nanoparticles; Hypericin; Ovarian cancer; *In vitro*; Drug delivery system**1. Introduction**

Ovarian carcinoma is the fourth most frequent cause of cancer-related death in women in the United States (Jemal et al., 2005). Approximately 22,000 new cases of ovarian cancer are diagnosed each year and 16,000 per year die from this disease. Ovarian cancer is often called the “silent killer” because symptoms observed in the early stages are not easily connected to the disease (Goff et al., 2000). Thus, almost 70% of diagnosed women already show extended growth of malignant cells corresponding to stages III and IV of the disease (Heintz et al., 2001). The currently recommended treatment is a combination of surgery followed by chemotherapy. However, ovarian cancer is characterized by the development of peritoneal micrometastases, which are not always removed by this standard treatment, mainly because micrometastases remain undetected by the con-

ventional detection methods. As a consequence, up to 50% of treated patients have a relapse and will inevitably die from their disease. The relative 5-year survival rate varies considerably with the disease stage at the moment of diagnosis. For patients diagnosed with stage I, the 5-year survival rate is 94%, compared to 19% for those diagnosed with stage IV (Gloeckler Ries et al., 2003). A photodynamic approach has been suggested to improve diagnostic and therapeutic methods, offering the opportunity of early detection and more effective eradication of peritoneal micrometastases (Allison et al., 2005).

Photodetection (PD) and photodynamic therapy (PDT) are based on the administration of drugs known as photosensitizers (PS) that are preferentially taken up and/or retained by malignant tissues (Sharman et al., 1999; Lange, 2003; Castano et al., 2004). The PS alone is harmless and ideally has no effect on either healthy or abnormal tissues. Illumination with light at the appropriate wavelength and dose induces either fluorescence allowing the detection of diseased tissues or photochemical reactions that result in tissue destruction. For several years, PD and PDT have been widely investigated in the field of cancer or other diseases

* Corresponding author. Tel.: +41 22 379 6573; fax: +41 22 379 6567.
E-mail address: Florence.Delie@pharm.unige.ch (F. Delie).

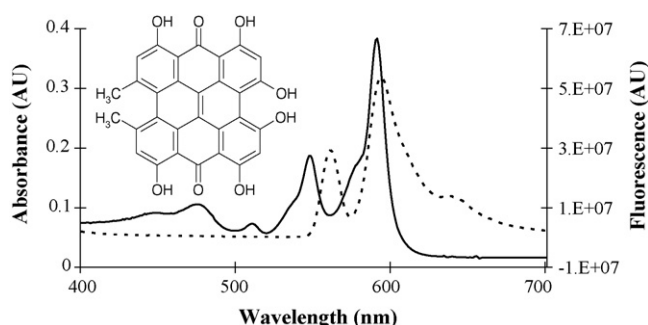


Fig. 1. Chemical structure, absorption (—) and emission (---, excitation at 280 nm) spectra of hypericin (Mw = 504.46) dissolved in ethanol (2.5 µg/ml).

such as age-related macular degeneration (AMD) (Hooper and Guymer, 2003). The interest of PD and PDT for ovarian cancer has been shown with 5-aminolevulinic acid and its derivatives *in vivo* in the NuTu-19 epithelial ovarian cancer model (Major et al., 1997; Chan et al., 2002; Ludicke et al., 2003).

The first-generation of photosensitizers suffered from several limitations such as poor selectivity, needs of large amounts of drug to obtain good efficiency, high cutaneous photosensitivity, widely limiting their clinical applications (Hopper, 2000). Thus numerous so-called second- and third-generations of PS were developed. Hypericin (Hy) is a natural compound belonging to the class of phenanthroperylenequinones (Fig. 1) and is extracted from the plant *Hypericum perforatum* found in Europe, North America, North Africa and some regions of Asia (Lavie et al., 1995; Agostinis et al., 2002). Its photodynamic activity was identified as a result of hypericium or photopoisoning induced in grazing animals consuming large quantities of plants containing this compound. One of the advantages of Hy is its large absorption spectrum with two major peaks at 545 and 590 nm (Fig. 1). Hy is not only a potent photosensitizer for PDT but also a fluorescent compound of potential interest for PD. Hy has been widely used in plant extracts as an anti-depressant. This treatment can be taken orally at a relative high dose (500 mg/day of extract corresponding to about 1–2 mg Hy/day) without major side effects. Its relative safety has further prompted interest in the use of Hy as a potential therapeutic tool for PDT and PD. The photoactivity of Hy has been demonstrated on different cancer cell models (Vandenbogaerde et al., 1997, 1998; Liu et al., 2000). Several reports have also shown Hy to be effective *in vivo* on mouse cancer models (Chen and de Witte, 2000; Chen et al., 2001; Du et al., 2003) and in humans to detect bladder cancer with a high sensitivity and specificity (D'Hallewin et al., 2002). As Hy has been shown to be efficient *in vitro* and *in vivo* for the detection or treatment of other cancers, Hy could also be a potent tool for the treatment and detection of ovarian cancer.

As most photosensitizers, Hy is characterized by a high lipophilicity. Although interesting with respect to the selectivity for neoplastic tissue (Lin, 1991), the resulting insolubility in physiologically acceptable media makes the systemic administration of conventional PS problematic and restricts their medical applications (Konan et al., 2002; Castano et al., 2005). To overcome this limitation, PS have been associated to colloidal carriers such as liposomes, emulsions, microparticles or

nanoparticles as reviewed by Konan et al. (2002). The interest in nanocarriers such as polymeric nanoparticles (NPs) to enable the production of an injectable suspension of PS has been increasing over recent years. NPs made of a polymeric matrix are a very stable and biocompatible drug delivery system. A large variety of materials and manufacturing processes can be used to produce NPs. This delivery system has already been shown to be effective in the field of PDT. Indeed, meso-tetra(*p*-hydroxyphenyl)porphyrin (pTHPP)-loaded NPs induced even a better photoactivity than free drug *in vitro* on mammary tumour cells (Konan et al., 2003a) and in the *in vivo* chick chorioallantoic membrane model (Vargas et al., 2004). Thus, polymeric NPs seem to be an interesting concept for Hy delivery.

Our objectives were first to produce Hy-loaded NPs using different polymers derived from polylactic acid (PLA) and to characterize them in terms of size, charge and drug loading. The phototoxicity of the encapsulated Hy was evaluated on the ovarian cancer cell model derived from Fischer 344 rats (Rose et al., 1996). This study was focused on the influence of PDT parameters such as drug concentration, incubation time and light dose as well as carrier characteristics such as nature of polymer and drug loading on the phototoxicity of Hy.

2. Materials and methods

2.1. Materials

Poly(lactic acid) (PLA) (Medisorb® Mw = 100 kDa) was obtained from Medisorb Technologies (Cincinnati, Ohio, USA). Poly(lactic-co-glycolic) acid (PLGA) with a lactic to glycolic ratio of 50:50 (Resomer® RG504, Mw = 48 kDa and RG502, Mw = 12 kDa) were received from Boehringer Ingelheim (Ingelheim, Germany). Hypericin (purity ≥ 98%) was provided by Alexis Corporation (Lausen, Switzerland). A stock solution of Hy was prepared in ethanol at 4 mg/ml and stored at –20 °C in the dark. Just before the *in vitro* experiments, dilutions were freshly prepared in complete culture medium. Poly(vinyl alcohol) (PVAL) (Mowiol 4–88) from Hoechst (Frankfurt/M, Germany) was used as a surfactant. D(+)-Trehalose dihydrate (Sigma Chemical, St. Louis, MO, USA) was used as a lyoprotectant. All other chemicals were of analytical grade.

2.2. Methods

2.2.1. Nanoparticle preparation

The nanoparticles were produced by the nanoprecipitation method. Typically, an organic phase containing 150 mg of polymer dissolved in 10 ml of acetone was poured under magnetic stirring into 20 ml of aqueous PVAL solution (0.4%, w/w). To obtain Hy-loaded NPs, a known amount of drug was first added to the organic phase. The organic solvent was evaporated under atmospheric pressure at room temperature. Afterwards, the NPs were purified by centrifugation (Beckman, Avanti™ 30, Fullerton, CA, USA), three times at 34,000 × *g* in order to remove the surfactant. Finally, after adding 30 mg of trehalose, NPs were freeze-dried (Edwards, Modulyo, Oberwil, Switzerland) and stored at +4 °C until use.

2.2.2. Nanoparticle characterization

NPs were characterized in terms of size, charge and drug loading. The mean size was determined by photon correlation spectroscopy using a Zetasizer[®] 5000 (Malvern instruments, UK). The NP size and shape were also checked by scanning electron microscopy (JEOL JSM-6400, Jeol Ltd., Japan). The zeta potential was measured in 10^{-3} M NaCl using the electrophoretic mode with the Zetasizer[®] 5000.

The drug loading was determined by reversed-phase HPLC after solubilization of NPs in acetone. For this purpose, an HPLC method was developed using a C8 column (4.6 mm \times 150 mm, 5 μ m, Agilent Technologies). The flow of the mobile phase composed of MeOH:H₂O (90:10) and 0.1% formic acid was set at 1 ml/min. Five microliters of sample were injected via an automatic injector (W717 plus Autosampler Waters, MA, USA). Hy was detected at 590 nm (W2487 Dual λ Absorbance Detector, Waters, MA, USA). Millennium[®] 32 chromatography manager software (Version 3.2) was used for peak integration. First, a calibration with standard solutions of neat Hy in ethanol was performed. Under these conditions, the retention time of the Hy was around 10 min. The presence of polymer did not influence retention parameter of Hy.

The residual PVAL was determined using a method based on the formation of a stable complex of PVAL with iodine in presence of boric acid (Konan et al., 2003b). Briefly, 5 mg of freeze-dried NPs were redispersed in 5 ml of 2N NaOH under stirring and the solution was neutralized with 2N HCl after complete hydrolysis of the polymer. This solution (1.6 ml) was added to 6 ml of boric acid (4%) and 1.2 ml of iodine solution (1.27% iodine and 2.5% potassium iodide in water). The absorbance of the solution was measured at 644 nm and the residual PVAL was evaluated using a calibration curve of PVAL standards.

2.2.3. *In vitro* phototoxicity

2.2.3.1. Cell line. The NuTu-19 cell line is a poorly differentiated Fischer 344 rat-derivative epithelial ovarian cancer cell line (Rose et al., 1996). Cells were maintained in DMEM medium (Gibco Life Technologies, Carlsbad, USA) supplemented with 10% fetal calf serum (FCS, Brunschwig, Amsterdam, the Netherlands) and 100 U/ml penicillin–streptomycin (Gibco Life Technologies) at 37 °C in a 5% CO₂ atmosphere.

2.2.3.2. Phototoxicity assay. Typically, NuTu-19 cells were seeded on 96 well plates at 1.5×10^4 cells per well in 100 μ l of culture medium and incubated for 24 h at 37 °C. The cells were washed and incubated with Hy in culture medium, free or loaded in NPs, for one hour at 37 °C. Then, the cells were washed and irradiated for 15 min (2.3 J/cm²). Irradiation was performed on the top of a box composed of 8 halogen tubes placed underneath a cooling compartment filled with circulating water to prevent possible heat-induced cell damages. Cell death was assessed by the 3-(4,5-dimethylthiazol-2-yl)-2,5-diphenyltetrazolium bromide assay (MTT, Sigma Steinheim, Germany) (Konan et al., 2003a). This assay is based on the reduction of the soluble MTT to a purple, insoluble formazan produced by mitochondrial dehydrogenases present only in living, metabolically active cells. Briefly, after washing, 50 μ l

of MTT solution (1 mg/ml) were added to each well and incubated for 3 h. The resulting formazan crystals were dissolved in 200 μ l of DMSO and the absorption was measured at 595 nm by means of a microplate reader (Model 550, Bio-RAD, Hercules, CA). Comparison of mean optical density 24 h after PDT between untreated (100%) and treated cells allowed the evaluation of phototoxicity of Hy-loaded nanoparticles compared to free drug. The influence of different parameters on the photoactivity *in vitro* was investigated by varying (i) Hy concentration from 0.01 to 0.2 mg/l; (ii) incubation time of cells with Hy formulations (15 min to 4 h); (iii) light dose (0.8–3.1 J/cm²) and (iv) NP drug loading (0.03–0.15%, w/w).

2.2.3.3. Statistical analysis. Values of cell viability are expressed as the mean \pm S.E. and the significance of the differences was calculated by Student's *t* test. Values of *P* < 0.05 were considered as significant.

2.2.4. *In vitro* hypericin release

The *in vitro* release of Hy from NPs was studied in the cell culture medium consisting of DMEM medium (Gibco Life Technologies) supplemented with 10% FCS (Brunschwig) and 100 U/ml penicillin–streptomycin (Gibco Life Technologies). Loaded NPs were suspended in 5 ml of medium to obtain a concentration of 5 mg/l of Hy. The suspension was distributed in five Eppendorf tubes of 1 ml. The tubes were shaken horizontally at 100 U/min at 37 °C (GFL shaking incubator, Burgwedel, Germany). At particular time intervals, the tube was centrifuged at $34,000 \times g$ for 5 min. The Hy concentration in the supernatant was determined by reversed-phase HPLC with fluorescence detection. The flow rate of mobile phase (MeOH/H₂O, 90:10, 0.1% formic acid) through the C8 column (4.6 \times 150 mm, 5 μ m, Agilent Technologies) was set at 1 ml/min (LC-pump LaChrom L-7100, Merck). Five microlitres of each sample were injected via an automatic sample injector (LaChrom L-7200, Merck). The fluorescence intensity of the samples was determined at 590/640 nm (excitation/emission) with a LaChrom L-7480 fluorescence detector. In these conditions, the retention time of Hy was about 10 min. The peaks were integrated with the appropriate software (HSM D-7000, version 4.1, Merck).

3. Results

3.1. Nanoparticle preparation and characterization

To evaluate the effect of the nature of the polymer on Hy photoactivity (molecular weight and lactic to glycolic ratio), three polymers were selected: one PLA polymer with a molecular weight of 100 kDa and two PLGA polymers with the same lactic acid to glycolic acid ratio (50:50) but different Mw (RG502 12 kDa and RG504 48 kDa). However, the nature of the polymer did not significantly influence NP characteristics as shown in Table 1. The nanoprecipitation method led to NPs of diameter in the range of 200–300 nm with a satisfactory polydispersity index (PI < 0.1). The zeta-potential was negative but close to 0 (>–8 mV) for all formulations. Low entrapment efficiencies

Table 1
Characterization of hypericin-loaded nanoparticles

Batch #	Polymer	Actual drug loading (% w/w)	Size (nm) (PI [*])	Zeta potential (mV)	Residual PVAL (% w/w)	Theoretical drug loading (% w/w)	Entrapment efficiency (% w/w)
1	PLA	0.03	265.5 (0.085)	−5.3	4.6	0.07	47.9
2		0.06	244.3 (0.075)	−6.8	4.2	0.09	62.6
3		0.12	210.3 (0.102)	−4.9	6.9	0.20	47.6
4		0.15	268.9 (0.073)	−3.7	4.3	0.20	69.8
5	RG504	0.03	250.0 (0.078)	−7.9	4.4	0.20	15.4
6	RG502	0.03	220.8 (0.102)	−5.9	4.9	0.20	12.5

* Polydispersity Index.

were observed with PLGA and the entrapment efficiency was quite erratic when PLA was used.

As PVAL is reported to be non-biodegradable, its administration should be minimized as much as possible. For this purpose, a step of NP purification is needed. To verify the efficacy of purification, the residual PVAL on freeze-dried NPs was determined. More than 90% of the PVAL was eliminated by centrifugation (Table 1). A minimal residual amount of PVAL, constituting a thin hydrophilic layer, is necessary to help the redispersion of NPs after freeze-drying.

3.2. In vitro photoactivity of hypericin

In controls where NuTu-19 cells were incubated with unloaded NPs with concentrations up to 1 g/l, no toxicity was observed. Furthermore, no dark toxicity of Hy either free or encapsulated was detected and light irradiation alone was also harmless to the cells.

3.2.1. Influence of hypericin concentration and nature of polymer on in vitro phototoxicity

The photoactivity of Hy-loaded NPs made of three different polymers (loading = 0.03%, w/w, batches 1, 5 and 6) was compared to free drug. For all tested formulations, cell viability decreased with increasing Hy concentrations as shown in Fig. 2.

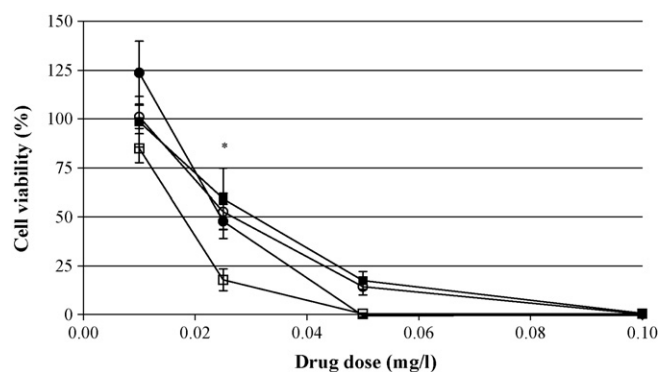


Fig. 2. Influence of drug concentration on photoactivity of free Hy (●) or Hy-loaded NPs (■: RG504; (○) RG502; (□) PLA; drug loading 0.03%, w/w). The NuTu-19 cells were incubated for 1 h, at equivalent drug doses ranging from 0.01 to 0.1 mg/l and irradiated at a light dose of 2.3 J/cm². MTT assay was performed 24 h after light exposure. Each data point represents the mean (±S.D.) of twelve values. *PLA Hy-loaded NPs showed a photoactivity significantly higher than free Hy (Student's *t*-test, *p* < 0.05).

Hy doses of up to 0.1 mg/l led to 100% cell death, regardless of the formulation. PLA NPs exhibited a higher photoactivity than PLGA NPs and free drug. At a drug concentration of 0.025 mg/l, Hy-loaded PLA NPs (0.03%) exhibited a 3-fold higher activity than free drug and PLGA NPs. Consequently, further experiments were carried out with PLA NPs.

3.2.2. Influence of the incubation time and light dose on phototoxicity

The influence of incubation time and light dose on Hy activity was evaluated at a concentration of 0.025 mg/l for incubation times ranging from 15 min to 2 h and light doses from 0.8 to 3.1 J/cm². The photoactivity of PLA Hy-loaded NPs was compared to free Hy. For both investigated formulations, photoactivity increased with increasing incubation times and/or light doses (Figs. 3 and 4). At 0.025 mg/l, first signs of Hy activity, free or encapsulated, were observed after 30 min and a light dose of 2.3 J/cm² (Fig. 3). Under this light condition, 100% cell death was observed after 2 h-incubation for PLA NPs. The incubation time could be reduced further if higher light doses were applied (Fig. 4). Indeed, after 1 h-incubation with Hy-loaded NPs, a 4-fold increase in light dose induced a drop in cell viability from 90 to 5%. These experiments confirmed the improved efficiency of PLA loaded NPs compared to free Hy. A significant difference was observed after 1 h of incubation and light doses of 1.6 or 2.3 J/cm² (Fig. 4). After 1 h-incubation and light expo-

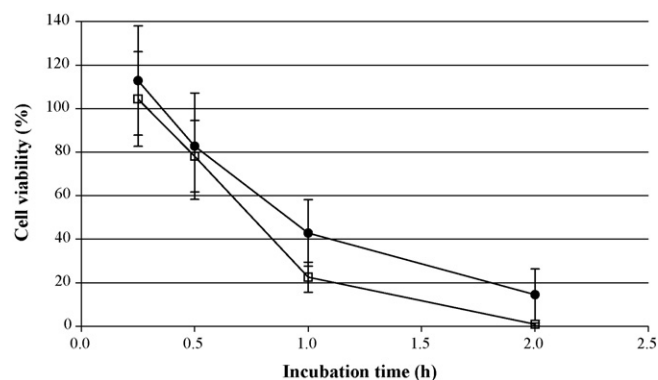


Fig. 3. Influence of incubation time on photoactivity of free Hy (●) or PLA Hy-loaded NPs (□, drug loading 0.03%, w/w). The NuTu-19 cells were incubated for increasing incubation times (from 15 min to 2 h), at an equivalent drug dose of 0.025 mg/l, and irradiated at a light dose of 2.3 J/cm². MTT assay was performed 24 h after light exposure. Each data point represents the mean (±S.D.) of 12 values.

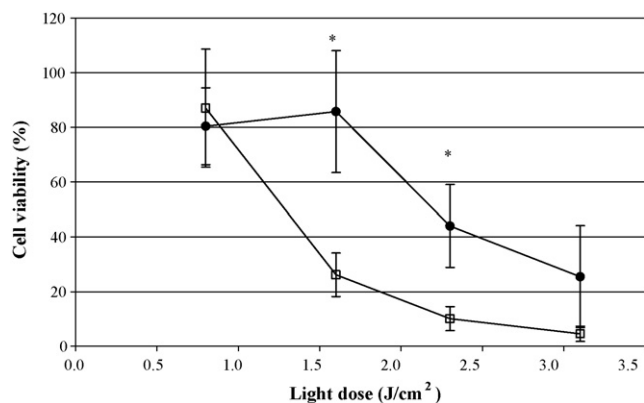


Fig. 4. Influence of light dose on photoactivity of free Hy (●) or PLA Hy-loaded NPs, drug loading 0.03%, w/w (□). The NuTu-19 cells were incubated for 1 h at an equivalent drug dose of 0.025 mg/l, and irradiated with increasing light doses (from 0.8 to 3.1 J/cm²). MTT assay was performed 24 h after light exposure. Each data point represents the mean (\pm S.D.) of 12 values. *PLA Hy-loaded NPs showed a photoactivity significantly higher than free Hy (Student's *t*-test, $p < 0.05$).

sure at 1.6 J/cm², PLA loaded NPs exhibited a 4-fold higher phototoxicity than free Hy.

3.2.3. Influence of drug loading on nanoparticle phototoxicity

As shown in Fig. 5, modulation of NP drug loading also influenced the cell death induced by PDT. NuTu-19 cells were incubated with four PLA NP batches with increasing drug loading (from 0.03 to 0.15% w/w, batches 1–4) at equivalent Hy doses of 0.025 and 0.1 mg/l. Interestingly, Hy efficiency decreased with increasing drug loading (Fig. 5). At 0.1 mg/l, NPs with a drug loading of 0.03% led to 100% cell death, whereas NPs at 0.15% killed less than 40% of the cells. The NPs at 0.06 and 0.12% showed a similar photoactivity on NuTu-19 cells.

3.2.4. Influence of nanoparticle drug loading on *in vitro* hypericin release

Fig. 6 shows the fractions of Hy released from NPs with increasing drug loading (from 0.03 to 0.15%, w/w) at different

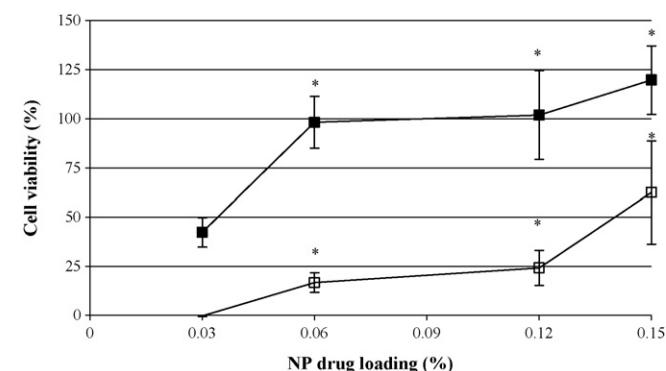


Fig. 5. Influence of drug loading on photoactivity of Hy-loaded PLA NPs. The NuTu-19 cells were incubated for 1 h, at equivalent drug concentrations of 0.025 (■) and 0.1 (□) mg/l, and irradiated at a light dose of 2.3 J/cm². MTT assay was performed 24 h after light exposure. Each data point represents the mean (\pm S.D.) of six values. *Significantly different from Hy-loaded PLA NPs at 0.03% (Student's *t* test, $p < 0.05$).

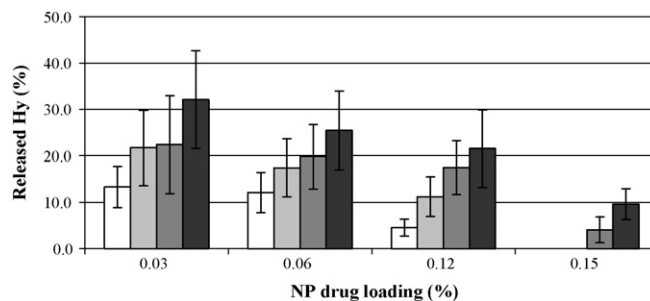


Fig. 6. Influence of drug loading on Hy release from loaded PLA NPs. NPs with increasing drug loading (0.03%, 0.06%, 0.12% and 0.15%) were shaken in DMEM medium supplemented with FCS and penicillin–streptomycin at 100 U/min at 37 °C. At particular time intervals (□: 10 min; ■: 60 min; ■: 180 min and ■: 1080 min), NPs were centrifuged and supernatants were analysed by HPLC ($n = 3$).

time intervals (0, 1, 3 and 18 h). At any given time, the fraction of released Hy increased when NP drug loading decreased. After 18 h of incubation, NPs with a drug loading of 0.15% released only 10% of Hy, whereas more than 30% of Hy was released from NPs with a drug loading of 0.03%. The initial burst was especially influenced by this drug loading. Indeed, NPs at a loading of 0.03% had already released nearly 15% of Hy at the beginning of the experiment, whereas NPs at 0.15% released no Hy before 3 h.

4. Discussion

For several indications, PDT and PD have been demonstrated to be efficient and advantageous over or in complement to other cancer therapies. However, some limitations still hamper their development in the clinic. The major problem is related to the delivery of mostly lipophilic PS to malignant tissues. PS lipophilicity makes formulation difficult due to the lack of physiologically acceptable solvents, especially when intravenous administration is considered. Therefore, the design of adequate PS delivery systems is critical for improving the outcome and acceptability of PDT and PD in a clinical context. Polymeric nanoparticles have been chosen as a possible means to overcome these delivery problems.

In this study, Hy-loaded NPs were produced with the following characteristics: (i) size in the 200–300 nm range to enable intravenous administration, (ii) negative zeta potential (> -8 mV), (iii) low residual PVAL and (iv) drug loading from 0.03 to 0.15% (w/w). Despite the hydrophobicity of Hy, poor entrapment efficiency was obtained when PLGA was used ($< 20\%$). The presence of hydroxyl groups on the Hy molecule may explain these results. Ionization of Hy in aqueous media may hamper the Hy entrapment into NPs. Changing parameters such as volume and composition of aqueous or organic phase did not improve drug encapsulation (data not shown).

The *in vitro* results showed that Hy preserved its photoactivity after nanoencapsulation. The phototoxicity of Hy-loaded nanoparticles *in vitro* on NuTu-19 cells was observed to be concentration-dependent (Fig. 2). The phototoxic effect of Hy-loaded NPs is also dependent on the nature of the polymer

and more precisely on the lactic to glycolic ratio. Indeed, PLA loaded NPs were more efficient than PLGA NPs or free Hy. These results suggest a rapid release from PLGA NPs leading to very similar activity profile as observed with the free drug. The beneficial effect of PLA NPs was mainly highlighted at a Hy concentration of 0.025 mg/l. Thus, encapsulation of PS into PLA NPs (loading = 0.03%, w/w) will be advantageous, as the same photodynamic effect could be obtained with a lower concentration of Hy, thus minimising possible side effects. Konan et al. (2003a) also observed concentration-dependant photoactivity of pTHPP in solution and loaded nanoparticles (PLA or PLGA) on EMT-6 mammary tumour cells. The photoactivity of pTHPP was enhanced by encapsulation regardless of the polymer used. *In vitro* NP photoactivity was ranked in the order: 50:50 PLGA > 75:25 PLGA > PLA. In this case, NPs possessing the same characteristics in terms of polymer molecular weight, particle size and drug loading, the copolymer molar ratio was the main parameter influencing the drug release and thus the activity. However, other parameters may influence the photodynamic response and modify this order. Our NPs were made of polymers having different molecular weight and were also less loaded (0.03 versus 8%, w/w), which induced a different distribution of the drug inside NPs and thus different photoactivity. Moreover, under these conditions, Hy may be active inside the NPs without previous release. Bourdon et al. (2000) studied the effect of meta-tetra(hydroxyphenyl)chlorin (mTHPC) in solution or entrapped on HT29 human adenocarcinoma cells. However a different drug delivery system, PLA nanocapsules (NCs) was used and their main goal was to study the interest of coating NCs with poloxamer or polyethylene glycol (PEG).

The different efficacy of PS formulations could be explained by the different cellular uptake pathway or rate depending on whether it is encapsulated or free. The mechanism of PS uptake by cells determines their subcellular localization and ultimately their photodynamic efficacy. Encapsulation may thus modify intracellular distribution into the different compartments of the cell bringing the PS closer to the targets. A specific subcellular localization could determine the mechanism of cell death. For example, localization in mitochondria has been associated with the tendency of PS to induce apoptosis (Castano et al., 2004). In solution, free PS are generally taken up by diffusion leading to a low intracellular concentration. In contrast, nanoparticles are taken up by endocytosis leading to higher accumulation of deliverable drug. This was further demonstrated in a recent publication where the degree of internalization of pTHPP-loaded nanoparticles sharply dropped when incubation was performed at +4 °C whereas no effect on the uptake of the free drug was observed (Konan et al., 2003c). Thus, an energy-dependent process is involved in the uptake of loaded-nanoparticles. Endocytosis of NPs leads to higher intracellular concentration whereas free pTHPP, due to its hydrophobic nature, tends to diffuse passively into the cell membrane, where it is less active. Therefore, encapsulation favours the PS internalization and thus, its photoactivity. On the other hand, other PS, which are less hydrophobic or too polar to diffuse through the plasma membrane are taken up, similarly to NPs, by endocytosis. In this case, such a difference in photoactivity between free and entrapped drug

may not be observed. Hy photoactivity also increased gradually with incubation time (Fig. 3). The effect of incubation time may be related to the kinetic of Hy uptake by cells. As PLA NPs are efficient at shorter incubation times, a rapid uptake by cells can be assumed. As observed by Konan et al. (2003a), in addition to the influence of incubation time, the phototoxic effect of PS can be enhanced by increasing the light dose (Fig. 4).

Increasing the NP drug loading had a negative effect on their photoactivity on NuTu-19 cells. Indeed and surprisingly, the higher the drug loading, the lower was the phototoxic effect (Fig. 5). This influence of drug loading could be explained by different parameters. An important parameter is the physical distribution of Hy in the polymeric matrix. For instance, in NPs of low drug loading, Hy might be closer to the surface and therefore more rapidly available for PDT. The drug release kinetics from NPs confirmed the negative effect of drug loading on NP activity. When the NP drug loading decreased, the Hy release was faster (Fig. 6). This trend was also observed by Mu and Feng (2003) with paclitaxel-loaded PLGA NPs of about 400 nm. After 1 month, the fraction of released paclitaxel was about 30, 8 and 5% for PLGA NPs with a drug loading of 2, 6 and 12%, respectively. For NPs of the same size, increasing the drug loading means a more compact structure or aggregation of drug. The main mechanism of release is diffusion of drug through the polymer matrix. However, in highly loaded NPs, the penetration of water enabling diffusion can be hampered, which could be the reason for the slower drug release observed at high drug to polymer ratio. Gorner et al. (1999) also studied the influence of drug loading (7, 13 and 30%, respectively) on the release of lidocaine from nanospheres (NS). But they stacked the influence of drug loading with the influence of size, using NS of increasing size (247, 366 and 817 nm respectively). The low-loaded, small-sized particles released the drug more rapidly and over a few hours, 35% of the initial drug amount was released. The larger NS exhibited a slower release, over about 15 h for NS of 366 nm and 24–30 h for NS of 817 nm, with equilibrium values of 30 and 24%, respectively. The influence on release profiles was a combination of size and drug loading. These authors suggested the formation of a heterogeneous matrix in highly loaded particles containing small crystals of lidocaine. Thus, the drug must first dissolve and then diffuse to the outer solution, resulting in slower release. To the best of our knowledge, no publication was found in the current literature that investigates the influence of drug loading on *in vitro* activity on tumour cells.

The photophysical properties of Hy might change in response to its environment. Among other factors, they will depend on the aggregation state of Hy. Hy may form aggregates in aqueous solution or even in some nonpolar solvents such as hexane and toluene (Wynn and Cotton, 1995; Huygens et al., 2005). Hypericin builds hydrogen bonds to other Hy molecules through the carbonyl and the phenolic hydroxyl groups. These bonds lead to stacked homoassociates up to five units, which exhibit a weak fluorescence resulting in a lower activity (Falk and Meyer, 1994; Etzlstorfer and Falk, 2000). This aggregation has been observed in PAM212 murine keratinocytes when incubated with high Hy concentrations (Theodossiou et al., 2004). The uptake of Hy by cells was measured by following

fluorescence during incubation time. When incubated with 5 μ M of Hy, the cell fluorescence increased regularly during the period of incubation time. At 50 μ M, the intracellular fluorescence did not increase with incubation time. However, an increasing fluorescence was recovered after extraction of Hy with DMSO, which suggests the intracellular aggregation of Hy. This quenching of fluorescence by aggregation hampered the *in vitro* phototoxicity. Thus, the non-fluorescent aggregates exert poor phototoxicity on cells. In our case, the Hy in highly loaded NPs was more concentrated. Hy aggregation could thus occur in these NPs, characterized by a quenching of fluorescence. This aggregated state could explain the inverse relationship between loading and photoactivity on NuTu-19 cells.

5. Conclusion

This study provides an *in vitro* proof of concept for using Hy-loaded NPs for PDT. Nanoencapsulation of Hy in PLA enhanced its *in vitro* activity, thus enabling the use of lower drug doses. The photoactivity was dependent on carrier parameters, such as the nature of the polymer and drug loading, as well as on PDT parameters such as incubation time, light dose and drug concentration. Low drug loading was required to obtain a better activity after PDT on NuTu-19 cells. To further clarify the influence of NP drug loading on Hy photoactivity, in depth photochemical characterization will be needed. The activity of Hy-loaded NPs will be investigated *in vivo* on Fischer rats bearing ovarian tumours. Photoactivity *in vitro* depends mainly on the photochemical and cell-penetrating properties of the Hy-loaded NPs, whereas *in vivo* activity is governed by many other factors such as pharmacokinetics and tissue distribution of the NPs, which are affected by the interaction with plasma and tissue components.

Acknowledgement

Dr. A. Major is gratefully acknowledged for providing the NuTu-19 cells and discussion.

References

- Agostinis, P., Vantieghem, A., Merlevede, W., De Witte, P.A.M., 2002. Hypericin in cancer treatment: more light on the way. *Int. J. Biochem. Cell. Biol.* 34, 221–241.
- Allison, R.R., Cuenca, R., Downie, G.H., Randall, M.E., Bagnato, V.S., Sibata, C.H., 2005. PD/PDT for gynecological disease: a clinical review. *Photodiagn. Photodyn. Ther.* 2, 51–63.
- Bourdon, O., Mosqueira, V., Legrand, P., Blais, J., 2000. A comparative study of the cellular uptake, localization and phototoxicity of meta-tetra(hydroxyphenyl) chlorin encapsulated in surface-modified submicronic oil/water carriers in HT29 tumor cells. *J. Photochem. Photobiol. B* 55, 164–171.
- Castano, A.P., Demidova, T.N., Hamblin, M.R., 2004. Mechanisms in photodynamic therapy: part one-photosensitizers, photochemistry and cellular localization. *Photodiagn. Photodyn. Ther.* 1, 279–293.
- Castano, A.P., Demidova, T.N., Hamblin, M.R., 2005. Mechanisms in photodynamic therapy: part three-photosensitizer pharmacokinetics, biodistribution, tumor localization and modes of tumor destruction. *Photodiagn. Photodyn. Ther.* 2, 91–106.
- Chan, J.K., Monk, B.J., Cuccia, D., Pham, H., Kimel, S., Gu, M., Hammer-Wilson, M.J., Liaw, L.H., Osann, K., DiSaia, P.J., Berns, M., Tromberg, B., Tadir, Y., 2002. Laparoscopic photodynamic diagnosis of ovarian cancer using 5-aminolevulinic acid in a rat model. *Gynecol. Oncol.* 87, 64–70.
- Chen, B., de Witte, P.A., 2000. Photodynamic therapy efficacy and tissue distribution of hypericin in a mouse P388 lymphoma tumor model. *Cancer Lett.* 150, 111–117.
- Chen, B., Xu, Y., Roskams, T., Delaey, E., Agostinis, P., Vandenheede, J.R., De Witte, P., 2001. Efficacy of antitumoral photodynamic therapy with hypericin: relationship between biodistribution and photodynamic effects in the RIF-1 mouse tumor model. *Int. J. Cancer* 93, 275–282.
- D'Hallewin, M.A., Kamuhabwa, A.R., Roskams, T., De Witte, P.A.M., Baert, L., 2002. Hypericin-based fluorescence diagnosis of bladder carcinoma. *BJU Int.* 89, 760–763.
- Du, H.Y., Bay, B.H., Olivo, M., 2003. Biodistribution and photodynamic therapy with hypericin in a human NPC murine tumor model. *Int. J. Oncol.* 22, 1019–1024.
- Etzlstorfer, C., Falk, H., 2000. Concerning the association of hypericin tautomers and their hypericinate ions. *Monatshefte für Chemie/Chem. Monthly* 131, 333–340.
- Falk, H., Meyer, J., 1994. On the homo- and heteroassociation of hypericin. *Monatshefte für Chemie/Chem. Monthly* 125, 753–762.
- Gloeckler Ries, L.A., Reichman, M.E., Lewis, D.R., Hankey, B.F., Edwards, B.K., 2003. Cancer survival and incidence from the surveillance, epidemiology, and end results (SEER) program. *Oncologist* 8, 541–552.
- Goff, B.A., Mandel, L., Muntz, H.G., Melancon, C.H., 2000. Ovarian carcinoma diagnosis. *Cancer* 89, 2068–2075.
- Gorner, T., Gref, R., Michenot, D., Sommer, F., Tran, M.N., Dellacherie, E., 1999. Lidocaine-loaded biodegradable nanospheres. I: Optimization of the drug incorporation into the polymer matrix. *J. Control. Release* 57, 259–268.
- Heintz, A.P., Odicino, F., Maisonneuve, P., Beller, U., Benedet, J.L., Creasman, W.T., Ngan, H.Y., Sideri, M., Pecorelli, S., 2001. Carcinoma of the ovary. *J. Epidemiol. Biostat.* 6, 107–138.
- Hooper, C.Y., Guymer, R.H., 2003. New treatments in age-related macular degeneration. *Clin. Exp. Ophthalmol.* 31, 376–391.
- Hopper, C., 2000. Photodynamic therapy: a clinical reality in the treatment of cancer. *Lancet Oncol.* 1, 212–219.
- Huygens, A., Kamuhabwa, A.R., de Witte, P.A., 2005. Stability of different formulations and ion pairs of hypericin. *Eur. J. Pharm. Biopharm.* 59, 461–468.
- Jemal, A., Murray, T., Ward, E., Samuels, A., Tiwari, R.C., Ghafoor, A., Feuer, E.J., Thun, M.J., 2005. Cancer statistics, 2005. *CA Cancer J. Clin.* 55, 10–30.
- Konan, Y.N., Berton, M., Gurny, R., Allemann, E., 2003a. Enhanced photodynamic activity of meso-tetra(4-hydroxyphenyl)porphyrin by incorporation into sub-200 nm nanoparticles. *Eur. J. Pharm. Sci.* 18, 241–249.
- Konan, Y.N., Cerny, R., Favet, J., Berton, M., Gurny, R., Allemann, E., 2003b. Preparation and characterization of sterile sub-200 nm meso-tetra(4-hydroxyphenyl)porphyrin-loaded nanoparticles for photodynamic therapy. *Eur. J. Pharm. Biopharm.* 55, 115–124.
- Konan, Y.N., Chevallier, J., Gurny, R., Allemann, E., 2003c. Encapsulation of p-THPP into nanoparticles: cellular uptake, subcellular localization and effect of serum on photodynamic activity. *Photochem. Photobiol.* 77, 638–644.
- Konan, Y.N., Gurny, R., Allemann, E., 2002. State of the art in the delivery of photosensitizers for photodynamic therapy. *J. Photochem. Photobiol. B* 66, 89–106.
- Lange, N., 2003. Controlled drug delivery in photodynamic therapy and fluorescence-based diagnosis of cancer. In: Mycek, M.-A., Pogue, B.W. (Eds.), *Handbook of Biomedical Fluorescence*. Marcel Dekker, Inc., New York, NY, pp. 563–635.
- Lavie, G., Mazur, Y., Lavie, D., Meruelo, D., 1995. The chemical and biological properties of hypericin—a compound with a broad-spectrum of biological activities. *Med. Res. Rev.* 15, 111–119.
- Lin, C.W., 1991. Photodynamic therapy of malignant tumors—recent developments. *Cancer Cells* 3, 437–444.

- Liu, C.D., Kwan, D., Saxton, R.E., McFadden, D.W., 2000. Hypericin and photodynamic therapy decreases human pancreatic cancer in vitro and in vivo. *J. Surg. Res.* 93, 137–143.
- Ludicke, F., Gabrecht, T., Lange, N., Wagnieres, G., van den Bergh, H., Berclaz, L., Major, A.L., 2003. Photodynamic diagnosis of ovarian cancer using hexaminolaevulinate: a preclinical study. *Br. J. Cancer* 88, 1780–1784.
- Major, A.L., Rose, G.S., Chapman, C.F., Hiserodt, J.C., Tromberg, B.J., Krasieva, T.B., Tadir, Y., Haller, U., DiSaia, P.J., Berns, M.W., 1997. In vivo fluorescence detection of ovarian cancer in the NuTu-19 epithelial ovarian cancer animal model using 5-aminolevulinic acid (ALA). *Gynecol. Oncol.* 66, 122–132.
- Mu, L., Feng, S.S., 2003. PLGA/TPGS nanoparticles for controlled release of paclitaxel: effects of the emulsifier and drug loading ratio. *Pharm. Res.* 20, 1864–1872.
- Rose, G.S., Tocco, L.M., Granger, G.A., DiSaia, P.J., Hamilton, T.C., Santin, A.D., Hiserodt, J.C., 1996. Development and characterization of a clinically useful animal model of epithelial ovarian cancer in the Fischer 344 rat. *Am. J. Obstet. Gynecol.* 175, 593–599.
- Sharman, W.M., Allen, C.M., van Lier, J.E., 1999. Photodynamic therapeutics: basic principles and clinical applications. *Drug Discov. Today* 4, 507–517.
- Theodossiou, T., Spiro, M.D., Jacobson, J., Hothersall, J.S., Macrobert, A.J., 2004. Evidence for intracellular aggregation of hypericin and the impact on its photocytotoxicity in PAM 212 murine keratinocytes. *Photochem. Photobiol.* 80, 438–443.
- Vandenbogaerde, A.L., Cuveele, J.F., Proot, P., Himpens, B.E., Merlevede, W.J., de Witte, P.A., 1997. Differential cytotoxic effects induced after photosensitization by hypericin. *J. Photochem. Photobiol. B* 38, 136–142.
- Vandenbogaerde, A.L., Kamuhabwa, A., Delaey, E., Himpens, B.E., Merlevede, W.J., de Witte, P.A., 1998. Photocytotoxic effect of pseudohypericin versus hypericin. *J. Photochem. Photobiol. B* 45, 87–94.
- Vargas, A., Pegaz, B., Debefve, E., Konan-Kouakou, Y., Lange, N., Ballini, J.P., van den, B.H., Gurny, R., Delie, F., 2004. Improved photodynamic activity of porphyrin loaded into nanoparticles: an in vivo evaluation using chick embryos. *Int. J. Pharm.* 286, 131–145.
- Wynn, J.L., Cotton, T.M., 1995. Spectroscopic Properties of Hypericin in Solution and at Surfaces. *J. Phys. Chem.* 99, 4317–4323.